Determination of the molar mass of argon from high-precision acoustic comparisons

2017 Metrologia 54 339

(http://iopscience.iop.org/0026-1394/54/3/339)

IOP Publishing | Bureau International des Poids et Mesures Metrologia

Metrologia **54** (2017) 339–347 https://doi.org/10.1088/1681-7575/aa68c7

Determination of the molar mass of argon from high-precision acoustic comparisons

X J Feng[1], J T Zhang[1], M R Moldover[2], I Yang[3], M D Plimmer[4] and H Lin[1]

[1] National Institute of Metrology, Beijing 100029, People's Republic of China
[2] National Institute of Standards and Technology, Gaithersburg, MD 20899, United States of America
[3] Korea Research Institute of Standards and Science, Daejeon 34113, Republic of Korea
[4] Conservatoire National des Arts et Métiers, La Plaine-Saint Denis 93210, France

E-mail: zhangjint@nim.ac.cn

Received 16 January 2017, revised 19 March 2017
Accepted for publication 23 March 2017
Published 8 May 2017

Abstract

This article describes the accurate determination of the molar mass M of a sample of argon gas used for the determination of the Boltzmann constant. The method of one of the authors (Moldover *et al* 1988 *J. Res. Natl. Bur. Stand.* **93** 85–144) uses the ratio of the square speed of sound in the gas under analysis and in a reference sample of known molar mass. A sample of argon that was isotopically-enriched in ^{40}Ar was used as the reference, whose unreactive impurities had been independently measured. The results for three gas samples are in good agreement with determinations by gravimetric mass spectrometry; $(\langle M_{\text{acoustic}}/M_{\text{mass-spec}}\rangle - 1) = (-0.31 \pm 0.69) \times 10^{-6}$, where the indicated uncertainty is one standard deviation that does not account for the uncertainties from the acoustic and mass-spectroscopy references.

Keywords: molar mass, argon, acoustic gas thermometry, Boltzmann constant

(Some figures may appear in colour only in the online journal)

1. Introduction

Among the primary methods for the determination of the Boltzmann constant k_B, acoustic gas thermometry (AGT) is currently the most accurate [1–7]. Here, one measures thermodynamic temperature T by determining the speed of sound c in the gas, which is related to the average kinetic energy in the three degrees of freedom of a gas in thermal equilibrium. For a zero-density (ideal) gas, the Boltzmann constant k_B is connected to the square speed of sound c_0^2 via

$$k_B = \frac{c_0^2 M}{T\gamma_0 N_A}, \tag{1}$$

where M is the molar mass of gas; N_A is the Avogadro constant, and γ_0 the ratio of the heat capacity at constant pressure to heat capacity at constant volume. For a monatomic gas, γ_0 is independent of temperature and exactly equal to 5/3. Using equation (1), one can determine the k_B by AGT by measuring c_0^2, T, and M. Most AGT experiments use argon as the working gas due to its high molar mass, simple isotopic composition, and relative insensitivity of c_0^2 to the most common chemical impurities. A high molar mass implies low acoustic resonant frequencies of the sample gas in a resonator, distant from troublesome shell vibrational modes. Helium is an alternative sample gas, because of its monoisotopic composition opposite to three dominant isotopes for argon. Nevertheless, the higher density of argon leads to the larger quality factor and lower resonant frequencies of acoustics than helium at equal pressure. Natural argon consists of ^{40}Ar, ^{38}Ar, and ^{36}Ar, with approximate relative abundances of 0.9964, 0.0006, and 0.0030, by mole fraction. Because the relative abundances of ^{38}Ar and ^{36}Ar are lower than the relative abundances of the minor krypton and xenon isotopes, mass spectroscopy can determine argon's average molar mass with lower fractional uncertainties than it can determine the average molar mass of krypton or xenon. Some recent determinations of the k_B using Ar by AGT were found to disagree by more than their standard uncertainties [2, 4]. A possible cause of this disagreement is a slightly different value for the molar mass of the gas samples used in the respective experiments. To resolve the discrepancy,

a collaborative study of the samples was performed using two methods: acoustic resonance frequency ratios (hereafter Method I) at the Laboratorie Commun de Metrologie—Conservatoire National des Arts et Métiers (LNE-CNAM) and National Institute of Metrology (NIM), and gravimetric mass spectrometry (Method II) at the Korea Research Institute of Standards and Science (KRISS). In a previous paper [8], a concise description of the work performed at NIM was given. Here, the experiment is described more thoroughly and the analysis is refined with the benefit of hindsight, and the work is presented in a broader context with an eye to future applications.

The rest of the article is set out as follows. In section 2, we recall briefly the approach for the accurate determination of molar mass by Method I. We describe the chronology of gas samples amongst the participating laboratories in section 3, and the experimental apparatus and procedure used at NIM in section 4. The results are presented in section 5 together with a comparison of those using gravimetric mass spectrometry. In section 6, we update the result of mass spectrometry in one of the samples in the present work.

2. Principle

The principle of Method I was suggested in 1988 by one of the present authors [1]. As stated above, primary AGT determines the thermodynamic temperature T from measurements of square speed of sound c^2 in a low-density monatomic gas of molar mass M and pressure p. The deviations from low-density behavior can be described by the acoustic virial equation [9]

$$\begin{aligned} c^2 &= \frac{\gamma_0 RT}{M} + A_1(T)p + A_2(T)p^2 + \cdots \\ &= \frac{\gamma_0 RT_{\mathrm{TPW}}}{M}\left[1 + 7.12\times10^{-4}\left(\frac{p}{300\,\mathrm{kPa}}\right)\right. \\ &\quad \left. + 5.0\times10^{-5}\left(\frac{p}{300\,\mathrm{kPa}}\right)^2 + \cdots\right]. \end{aligned} \tag{2}$$

In equation (2), the factors $A_1(T)$ and $A_2(T)$ are related to the density virial coefficients and their temperature derivatives [9, 10]. The factor $A_1(T)$ accounts for the interaction of pairs of molecules, while $A_2(T)$ accounts for the interaction of triplets of molecules. The term $\gamma_0 RT/M$ is the ideal-gas limit corresponding to equation (1) with the universal gas constant R replacing $N_\mathrm{A}k_\mathrm{B}$. The second line of equation (2) displays the relative importance of $A_1(T)$ and $A_2(T)$ for argon at the temperature of the triple point of water ($T_{\mathrm{TPW}} = 273.16\,\mathrm{K}$) and $p = 300$ kPa, where we measured speed-of-sound ratios.

If the gas of two samples of molar mass M (to be determined) and M_r (the reference) are maintained at constant pressure and temperature, the ratio of their square speeds of sound is given by:

$$\frac{c^2}{c_\mathrm{r}^2} = \frac{M_\mathrm{r}}{M}\left\{1 + \frac{\Delta(MA_1)}{\gamma_0 RT}p + \left[\frac{\Delta(MA_2)}{\gamma_0 RT} - \frac{M_\mathrm{r}A_{1,\mathrm{r}}(T)\Delta(MA_1)}{(\gamma_0 RT)^2}\right]p^2 + \cdots\right\} \tag{3}$$

with $\Delta(MA_1) \equiv MA_1(T) - M_\mathrm{r}A_{1,\mathrm{r}}(T)$ and $\Delta(MA_2) \equiv MA_2(T) - M_\mathrm{r}A_{2,\mathrm{r}}(T)$, where $A_{1,\mathrm{r}}(T)$ and $A_{2,\mathrm{r}}(T)$ are corresponding factors related to the density virial coefficients of the reference gas. Because the reference gas and the unknown gas are so similar, the terms $\Delta(MA_1)$ and $\Delta(MA_2)$ are expected to be negligible. (In the appendix of this paper, we argue that $\Delta(MA_1)$ is very small.) Thus, one can determine the ratio of the molar masses of two argon samples with high accuracy by comparing their square speeds of sound at a constant temperature and pressure. Specifically, the molar mass of the gas under analysis is given by:

$$M = M_\mathrm{r}(c_\mathrm{r}/c)^2. \tag{4}$$

Equation (4) forms the basis of Method I.

3. Chronology of gas samples among participants and the experiment at NIM

To implement Method I, Moldover *et al* [1] used as a reference gas a commercially-purchased sample of argon that was isotopically-enriched in ^{40}Ar. We designate this reference gas 'Ar40'. Using a getter, they removed the chemically-reactive impurities from the Ar40 and they estimated that the relative uncertainty of the molar mass was $u_\mathrm{r}(M_{\mathrm{Ar40}}) = 0.7\times10^{-6}$ from the uncertainties of their measurements of the mole fractions of krypton X_{Kr} and xenon X_{Xe} impurities. (Throughout this paper, we report the statistical, standard uncertainty corresponding to a 68% confidence level.) In this work, we did not repeat the measurements of X_{Kr} and X_{Xe}, which contributed 0.7×10^{-6} to the relative uncertainty of M_{Ar40} in [1]. Thus, all our acoustic determinations of M, by comparison with M_{Ar40} via equation (4), have this additional uncertainty component.

Moldover *et al* [1] compared the square speeds of sound of the samples of the Ar40 reference to samples of the commercially-purchased working gas to establish the molar mass M_{Ar} of the working sample with respect to M_{Ar40} with the relative uncertainty $u_\mathrm{r}(M_{\mathrm{Ar}}) = 0.8\times10^{-6}$. Crucially, for the present work, they saved most of the reference gas in its original container. During recent determinations of the Boltzmann constant, the present authors used some of the reference gas to characterize the molar masses of samples of argon gas by Method I. Since the work of [1], AGT has benefitted from technological advances, and techniques have become so refined that a relative measurement uncertainty of a few parts in 10^7 for temperatures close to T_{TPW} is achievable. Moreover, square speeds of sound derived from frequencies of different acoustic modes are spread by fractional differences of only (2 to 5) $\times\,10^{-7}$, and so their ratio for two ideal gases can be obtained at a similar level of uncertainty. Such a level is comparable with that achieved using advanced mass spectrometry referenced to a standard reference gas mixture [8, 11, 12]. Thus, measurements using Method I can be compared to those using Method II and vice versa. If care is taken, then a sample studied by Method I can be recovered for study elsewhere i.e. the method is non-destructive.

The complementary determination of molar masses using Method II, gravimetric mass spectrometry, was undertaken at KRISS for a total of 15 samples, including the nine studied by LNE-CNAM and the one at NIM by Method I.

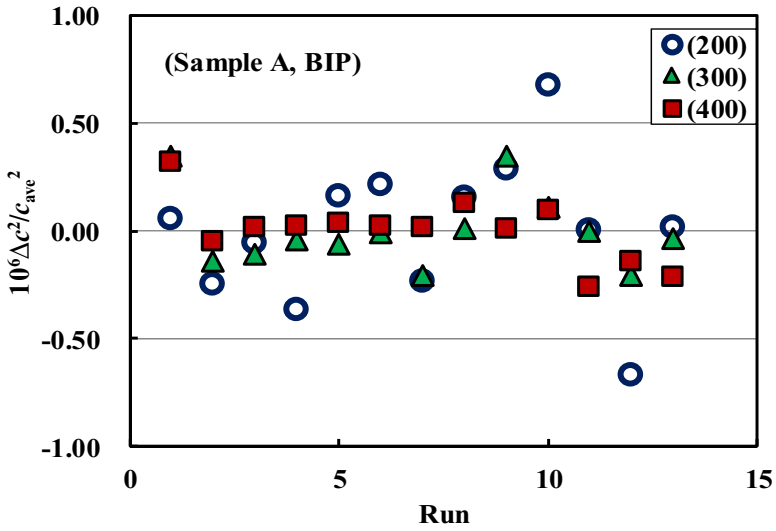

Figure 1. Relative deviations of square speeds of sound from their mean for Sample A.

The work is described in detail in Yang *et al* [8], and so we mention only a few key facts. Method II relies on the analysis of the individual abundances of the stable isotopes of argon, namely ^{36}Ar, ^{38}Ar, and ^{40}Ar. The mass spectrometry conducted at KRISS used reference mixtures prepared by gravimetric methods [8, 11, 12], where the isotopic ratios ^{40}Ar/^{36}Ar of the mixtures were determined by using two mass-comparators [11]. Thus, the procedure was 'primary' mass spectrometry. In contrast, certain mass spectrometry measurements of M_{Ar} [13] used local atmospheric argon as a reference mixture; these measurements assumed the relative isotopic abundances in atmospheric air were those reported by Lee *et al* [11]. In the remainder of this paper, we shall concentrate on the molar mass determination using square speeds of sound and compare the results with those from mass spectrometry.

In this work, we compared the sample of nearly monoisotopic Ar40 from [1] with three argon samples from Air Products[5]: Sample A of BIP grade and Samples B and C of BIP PLUS grade. We have described the properties of BIP and BIP PLUS in previous publications [7, 14].

One sample, designated 'A(1)', was collected from the same container as Sample A. In 2010, Sample A(1) was analyzed for M_{Ar} at KRISS using primary mass spectrometry calibrated with a reference mixture prepared by Lee *et al* [11]. A sample designated 'B' was from one container of BIP PLUS. We used another container of BIP Plus in this work and took three samples from this container. One of the three was labeled 'C' and analyzed with Method I. The second of the three was labeled 'C(1)' and sent to KRISS for analysis by primary mass spectrometry. The third was labeled 'C(2)' and sent to LNE-CNAM for acoustic analysis as one constituent of the nine samples mentioned in the literature [8]. Sample C(2) was finally delivered to KRISS for the analysis with Method II.

[5] In order to describe materials and procedures adequately, it is occasionally necessary to identify commercial products by manufacturers' name or label. In no instance does such identification imply endorsement by the authors' institutions, nor does it imply that the particular product or equipment is necessarily the best available for the purpose.

4. Experimental apparatus and procedure

The apparatus used here was adapted from that used for a determination of the Boltzmann constant. It has been described in detail elsewhere [7, 14]. Here, we concentrate on the aspects specific to the determination of molar mass. The molar mass measurements were carried out at T_{TPW}. We determined the squared ratio of the speeds of sound $(c_{Ar}/c_{Ar40})^2$ using the cylindrical cavity specially designed for the determination of the k_B [7]. It has a nominal length of 80 mm and a nominal inner diameter of 80 mm. The cylindrical shell is made of bearing steel. To allow an optical determination of the cavity length, the end-plates, 15 mm in thickness and 108 mm in diameter, are made of optical-quality fused silica. The working surface of each end-plate was coated with a partially-reflecting metallic film. A 10 mm diameter hole was ground out of the outside-facing surface of each end-plate to a depth of 14.70–14.75 mm leaving a silica diaphragm 0.25–0.30 mm thick that was flush with the working surface of the end-plates. The piezoelectric transducers (PZTs) were cemented to the outside surface of each diaphragm with epoxy resin.

A single duct for measuring and changing the pressure of argon gas led from the cavity to the gas manifold. The gas manifold was the same as the one used in earlier work [7]. It was assembled using all-metal connectors and valves with bellows stem seals. An SAES Model GC50 getter was installed for gas purification. Heating tapes were wrapped around the manifold to bake-out absorbed gases. Prior to baking, the SAES getter was preheated for 2 h to reach its operating temperature of 400 °C and it was maintained at 400 °C throughout the bake-out. In the experiment described here, the bake-out lasted more than 24 h during which the manifold was maintained at 100 °C, while it was alternately evacuated and purged with pure argon.

The temperature of the cavity was measured using two capsule-type standard platinum resistance thermometers (Hart 5686). Each thermometer was enclosed in a metal sleeve as previously described [7]. An ASL F900 bridge and a 100 Ω standard resistor (Tinsley 5685A) were used to measure the

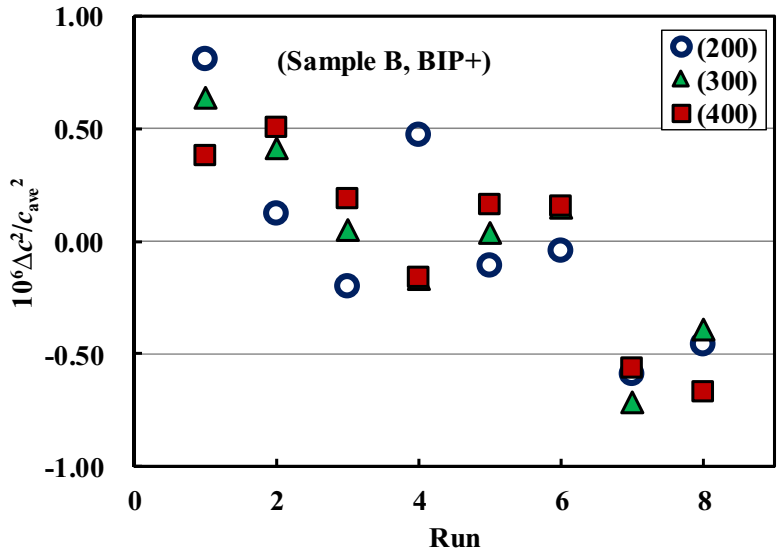

Figure 2. Relative deviations of square speeds of sound from their mean for Sample B.

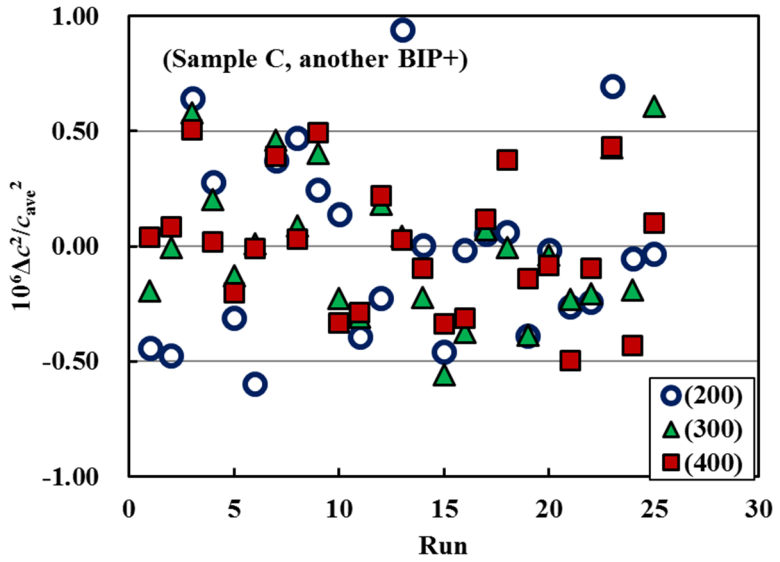

Figure 3. Relative deviations of square speeds of sound from their mean for Sample C.

resistance ratios of the thermometers. The thermostat maintained the temperature of the resonator within ±0.1 mK during the experiment.

Two PZTs were used for the generation and detection of sound. The source PZT was driven by a sinusoidal voltage generated by an Agilent 33220A waveform generator that was locked to a 10 MHz standard signal provided by a GPS clock. The detecting PZT was read with a two-phase lock-in amplifier (Stanford Research Systems SR830) locked to the driving voltage.

The pressure vessel surrounding the acoustic cavity was filled with BIP argon from a different container than the one used for Samples A and A(1). The surrounding pressure was 200–300 Pa below the pressure of the test gas inside the cylindrical cavity. This pressure difference ensured that outgassing from the transducers, epoxy resin, wire insulation, etc. located in the pressure vessel would not contaminate the test gas. A differential pressure gauge (MKS Baratron 616A) measured the pressure difference between the gases inside the cavity and the pressure vessel. The metal diaphragm of the differential pressure gauge isolated the cavity from the rest of the gas manifold. An absolute pressure gauge (Ruska 7250 xi, 0–600 kPa) was used to monitor the gas pressure within the pressure vessel. This procedure avoided contamination of the argon gas in the cavity by impurity release from the non-metal diaphragm of the absolute pressure gauge. The mating surfaces of the end-plates and the cylindrical shell were sufficiently flat that leakage of the pure argon gas from the cavity into the pressure vessel was negligible. The short-term drift of the absolute pressure gauge and the differential pressure gauge was measured of less than 20 Pa for both transducers. Supposing the worst case of 40 Pa drift occurring in the pressure measurement, the calculation from equation (2) indicates a fractional change of about 1×10^{-7} (0.1 ppm) for the squared sound of speed at 300 kPa. Thus, the drift of the pressure gauges causes negligible effect on the determination of the mole mass.

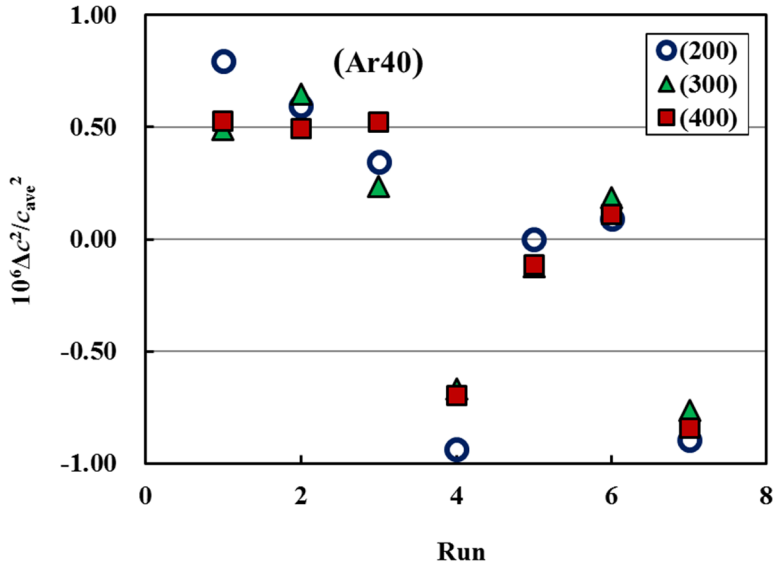

Figure 4. Relative deviations of square speeds of sound from their mean for the reference gas Ar40.

5. Speed-of-sound ratio measurements

We measured the square speeds of sound in the sequence of Sample A, Sample B, Sample C, and Ar40. The measurements were performed at a nominal gas pressure of 300 kPa and at the temperature T_{TPW}. The choice of pressure was governed by a trade-off between two sources of uncertainty: (1) as the pressure increases, the signal-to-noise ratio of the resonance frequency measurements improves, thereby reducing uncertainty, and (2) as the pressure increases, the coupling between the acoustic oscillations of the gas and the hard-to-calculate compliance of the shell grows, thereby increasing uncertainty.

The frequency perturbations from the shell's compliance cannot be calculated accurately, because they depend on the geometry of the acoustic oscillations, the geometry and elastic properties of the shell, and the difficult-to-model visco-elastic response of gas-filled, bolted joints. In [14], we showed that four classes of perturbations from the shell increase as a nearly-linear function of the argon pressure and that these perturbations have a complex frequency dependence that includes peaks at frequencies where the empty shell has mechanical resonances.

We determined three values of the speed-of-sound ratios $(c_{Ar}/c_{Ar40})^2$ using the three longitudinal acoustic modes (200), (300), and (400) that had resonance frequencies at 3.8, 5.7, and 7.6 kHz. For Samples A, B, and C, the fractional standard deviations of the three values of $(c_{Ar}/c_{Ar40})^2$ from their mean were 0.21×10^{-6}, 0.33×10^{-6}, and 0.27×10^{-6}, respectively. If the frequency-dependent compliance of the shell had a peak near one of these frequencies, we would expect larger inconsistencies among the three longitudinal modes.

The signal for the longitudinal mode (100) was too small to be useful, while longitudinal modes (500) and above were strongly perturbed by the shell's compliance. In the determination of speed of sound, only corrections to the perturbations caused by the thermal and the viscous boundary layer were applied to the measurements of resonant frequencies.

Table 1. Molar mass determinations using square speed-of-sound ratios in argon gas at 300 kPa at T_{TPW} using a cylindrical resonator. The average values of M_{Ar} are listed in table 3.

Sample	Mode	$10^6\left(\frac{c_{Ar}^2}{c_{Ar40}^2}-1\right)$	M_{Ar} (g · mol^{-1})
A	(200)	368.58	39.947 795
	(300)	368.98	39.947 779
	(400)	368.69	39.947 791
B	(200)	369.15	39.947 772
	(300)	369.77	39.947 748
	(400)	369.70	39.947 751
C	(200)	368.46	39.947 800
	(300)	368.97	39.947 779
	(400)	368.62	39.947 794
Ar-M[a]	(02)	368.21(13)	
	(03)	368.20(24)	
	(04)	368.16(23)	
	(05)	368.07(26)	
	(06)	368.08(23)	

[a] The ratios and standard deviations for Ar-M were obtained using a spherical resonator. (Appendix 3 of [1].) Frequency measurements near T_{TPW} and 103 kPa, 117 kPa, and 131 kPa were corrected for small temperature and pressure differences and then averaged.

The frequency-dependent perturbations of shell motions for mode (200), (300), and (400) are approximately identical for the sample and the reference gases to be cancelled out from the ratios of square speeds of sound.

Figure 1 shows the speed-of-sound ratio measurements for Sample A. The measurements were repeated for 13 runs. The values of speeds of sound scatter randomly around the average. The relative standard deviations are 0.33×10^{-6}, 0.18×10^{-6}, and 0.15×10^{-6} for modes (200), (300), and (400), respectively. The (200) mode shows the greatest scatter resulting from a lower signal-to-noise ratio than for (300) and (400).

Figure 2 shows the results of eight repeated measurements for Sample B. The first six measurements are tightly grouped, whereas the last two appear to diverge. The relative standard deviations are 0.46×10^{-6}, 0.43×10^{-6}, and 0.43×10^{-6} for modes (200), (300), and (400), respectively.

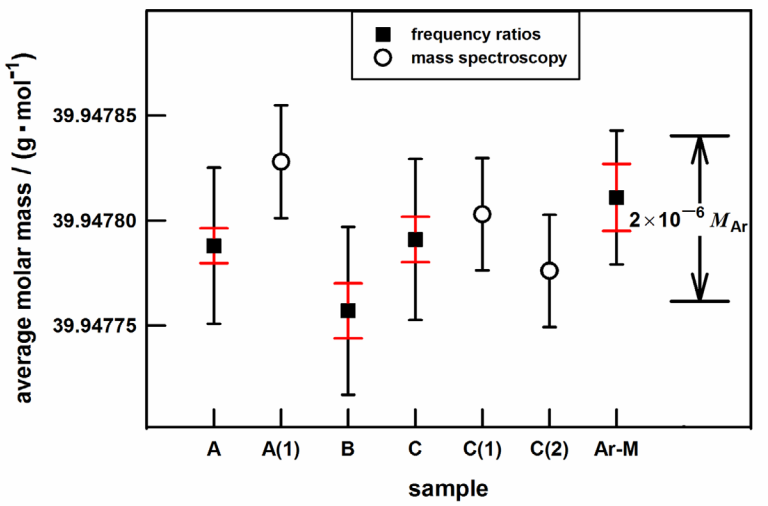

Figure 5. Molar masses from Methods I and II. For the frequency ratio data, the inner (red) uncertainty bars indicate the standard deviation of the ratios $(c_{Ar}/c_{Ar40})^2$ from their means and the outer uncertainty bars include the uncertainty of the reference gas $u(M_{Ar40})$.

Figure 3 shows the results for Sample C. The measurements were repeated for 25 runs. The data are scattered around the mean. The relative standard deviations are 0.40×10^{-6}, 0.31×10^{-6}, and 0.29×10^{-6}, respectively.

After the work on Sample C, we measured the speed of sound in the reference gas Ar40. Before the Ar40 measurements, we flushed the cavity with Ar40 three times for 20 min each, but only at pressures up to 15 kPa, because of the limited supply of Ar40. Perhaps this limited flushing is related to the larger dispersion of the values of $\Delta c^2/c^2_{ave}$ for Ar40 than for the other gases. The data shown in figure 4 have relative standard deviations of 0.68×10^{-6}, 0.55×10^{-6}, and 0.58×10^{-6} for modes (200), (300), and (400), respectively.

Using equation (4), we calculated the molar masses of Samples A, B, and C using the known molar mass of the reference gas Ar40. The calculation was carried out mode by mode. The calculations of all modes were then averaged to yield the molar mass of a particular sample with the results listed below in table 3. The ratios of the square speeds of sound were calculated and are listed in table 1 in the column labeled $10^6(c^2_{Ar}/c^2_{Ar40} - 1)$. Here, the subscript 'Ar' denotes the sample argon gas and the subscript 'Ar40' denotes the reference gas Ar40. Table 1 includes values of the molar mass of commercial argon Ar-M that are reported in appendix 3 of [1] using Method I with a spherical resonator.

The data in table 1 show that Samples A, C, and Ar-M have their average molar masses (see table 3) nearly identical and that their fractional differences are less than 0.07×10^{-6}. Sample B has the average molar mass -0.78×10^{-6} lower than Sample A. The average molar mass of Sample Ar-M is 0.57×10^{-6} larger than Sample A. The samples for the comparison originated from very different sources. For the four samples listed in table 1, the averages of the molar masses span the fractional range of 1.3×10^{-6}, which is comparable to the range (1.9×10^{-6}) spanned by the 15 samples reported in [8].

The molar mass of Sample A(1) collected from the same container as Sample A was analyzed with Method II at KRISS in 2010 [14]. The analysis with Method II had been carried out using as a reference the standard reference mixture prepared by Lee *et al* [11], and the result was updated to reflect new information (see section 6). Similarly, the molar mass of Samples C(1) and C(2), which was collected from the same container as Sample C, was analyzed by mass spectrometry at KRISS in 2014 [8]. The reference mixture is also based on the same preparation by Lee *et al* [11]. In figure 5, we compare the values of the molar masses of Samples A and A(1), B, C, C(1), C(2), and Ar-M with their standard uncertainty budget.

Table 2. Budget of relative uncertainties for the measurement of molar mass by Method I.

Uncertainty	Sample A	Sample B	Sample C
$10^6 u_r(M_{Ar40})$	0.70	0.70	0.70
$10^6 u_r(c^2_{Ar})$	0.23	0.42	0.33
$10^6 u_r(c^2_{Ar40})$	0.57	0.57	0.57
$10^6 u_r(M_{Ar})$	0.93	1.00	0.96

The fractional differences between the molar masses $(M_{C(1)} - M_C)/M_C$ and $(M_{C(2)} - M_C)/M_C$ were -0.30×10^{-6} and 0.37×10^{-6}, respectively. The value M_C obtained using Method I lies mid-way between the results of measurements with Method II. The results agree well and the differences are well covered by their claimed uncertainties. Besides, the difference between the results for Samples C(1) and C(2) illustrates that the measurements by Method II for the samples collected from the same container have the fractional difference of 0.67×10^{-6}. This is attributed to the different history of Samples C(1) and C(2) and the reproducibility of Method II. According to the analysis based on the intensive study in [8], $M_{A(1)}$ has to be decreased by 0.39×10^{-6} from its value given in 2010 [14]. Thus, the fractional difference $(M_{A(1)} - M_A)/M_A$ is updated to 1.00×10^{-6}. Given the uncertainty budgets for Methods I and II, the result cannot be deemed anomalous.

The uncertainties associated with the determination of the molar masses by Method I can be budgeted using equation (4). The equation shows that an uncertainty arising from two sources, the uncertainty for the molar mass of the Ar40 sample and the scattering levels of measuring speeds of

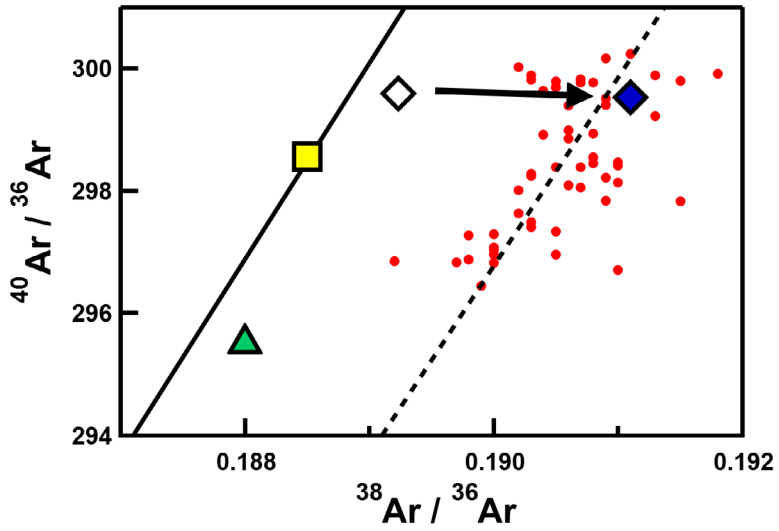

Figure 6. The updated gravimetric measurement on Sample A(1) replaced the open diamond with the filled diamond. The updated measurement is consistent with the 2014 (dashed) mass fractionation line. The triangle and square represent determinations of the composition of atmospheric argon by Nier [15] and Lee [11], respectively.

sound. Moldover *et al* [1] stated the relative standard uncertainty of 0.7×10^{-6} for determining the molar mass of the Ar40 sample. The relative standard deviation from the average of square speeds of sound for Samples A, B, C, and Ar40 were accounted for in the uncertainty sources. On consideration of the stated uncertainty sources, the relative standard uncertainty for deriving the molar mass of sample by equation (4) is given by:

$$u_r(M_{Ar}) = \sqrt{u_r^2(M_{Ar40}) + u_r^2(c_{Ar}^2) + u_r^2(c_{Ar40}^2)}\,. \qquad (5)$$

According to equation (5), we budgeted the uncertainties with deriving the molar masses of Samples A, B, and C in table 2.

6. Update of mass spectrometry measurements

In 2010, a sample of BIP grade argon from the same supply cylinder as Sample A was analyzed by the mass spectrometer at KRISS and the result was used for the 2011 measurement of the Boltzmann constant at NIM [14]. In this report, we label that Sample A(1). The isotopic concentration ratios of the argon determined from the mass spectrometer measurements at KRISS were ^{38}Ar/^{36}Ar = 0.1892, and ^{40}Ar/^{36}Ar = 299.59. From these ratios, the molar mass of Sample A(1) was determined in 2010 as (39.947 843 ± 0.000 028) g · mol^{-1}.

After the intensive analysis on the isotopic ratio of argon samples in 2014 [8], we identified two corrections that need to be applied to the 2010 mass spectrometry measurement of Sample A(1).

The first correction is from the misquoted value of ^{40}Ar/^{36}Ar in the previous analysis. In the 2010 work, the gravimetric value of ^{40}Ar/^{36}Ar of isotopic reference was mistakenly quoted as 330.37, instead of the correct value of 330.30, and the error propagated to the ratio of ^{40}Ar/^{36}Ar of the sample. The correct value of ^{40}Ar/^{36}Ar of Sample A(1) is then ^{40}Ar/^{36}Ar = 299.53. In terms of the molar mass, this correction amounts to the fractional decrease of 0.07×10^{-6}.

Table 3. Summary of results.

Sample	Method	Molar mass G · mol^{-1}	$10^6 \times u_r(M)$
A	Acoustic	39.947 788	0.93
A(1)	Mass spec.	39.947 828	0.70
B	Acoustic	39.947 757	1.00
C	Acoustic	39.947 791	0.96
C(1)	Mass spec.	39.947 803	0.70
C(2)	Mass spec.	39.947 776	0.70
Ar-M[a]	Acoustic	39.947 811	0.8

[a] Taken from table 10 in [1].

The second correction concerns how the mass discrimination correction K should be applied for the isotopic ratio ^{38}Ar/^{36}Ar. The non-zero K comes from the slightly different sensitivity of the mass spectrometer for different isotopes of argon. It is obtained by comparing ion current ratio I to the known isotopic concentration ratio R_{iso}, usually by the gravimetric method, of a reference isotopic sample, $K = (R_{iso}/I - 1)$. In our previous measurement in 2010, the mass discrimination corrections were calculated for ^{38}Ar/^{36}Ar and ^{40}Ar/^{36}Ar independently as $K_{38/36} = -0.0116$ and $K_{40/36} = -0.0035$, respectively. For this independent determination, KRISS used ion current measurements and gravimetric ratios of isotopic contents for both ^{38}Ar/^{36}Ar and ^{40}Ar/^{36}Ar.

However, in our campaign of 2014 measurements in which most of the present authors were involved, only $K_{40/36}$ was evaluated experimentally using the ion current and gravimetric ratios of ^{40}Ar/^{36}Ar of the isotopic reference. Then, under the assumption that the sensitivities of ^{36}Ar, ^{38}Ar, and ^{40}Ar vary linearly with the atomic number, $K_{38/36}$ was calculated as $K_{38/36} = K_{40/36}/2$. We chose this method, because the isotopic reference we used so far at KRISS is a binary mixture of ^{36}Ar and ^{40}Ar, and ^{38}Ar only exists in the reference as an isotopic impurity. Because the fractional amount of ^{38}Ar in the reference was too small (0.000 16 compared to 0.0006 in the atmospheric argon), we concluded that using the linearity assumption and obtaining the mass discrimination correction

of $K_{38/36}$ from $K_{40/36}$ would be a better choice. Therefore, we update $K_{38/36}$ as −0.0019 for our 2010 measurement. (Because of the first correction, we update $K_{40/36}$ as −0.0038 from −0.0035, and $K_{38/36}$ was calculated from the new $K_{40/36}$) This correction decreases the molar mass of Sample A(1) by the fractional amount of 0.31×10^{-6}.

Figure 6 represents the update of the isotopic ratios of Sample A(1). Also shown are the data points from the 2014 study (circles) [8] and the atmospheric argon composition by Nier (triangle) [15] and Lee (square) [11]. Two lines in the figure represent mass fractionation lines that pass through the Lee measurement (solid) [11], and the KRISS 2014 measurements (dashed) [8]. The updated value is within the spread of measurements from the fractionation line that represents the data set from the 2014 measurements, but the old value was closer to the fractionation of the two atmospheric argon measurements by Nier or Lee. The cause of the difference, as stated in [8], is unknown. Because of this lack of understanding, the relative uncertainty of 0.35×10^{-6} was added in quadrature to account for this unknown effect [8].

After these two corrections, our updated assessment of the isotopic contents of sample A using the mass spectrometer is $^{40}\mathrm{Ar}/^{36}\mathrm{Ar} = 299.53$ and $^{38}\mathrm{Ar}/^{36}\mathrm{Ar} = 0.1911$. From these ratios, the molar mass of Sample A(1) is 39.947 828 $\mathrm{g \cdot mol^{-1}}$. The relative change in the molar mass from our original evaluation in 2010 was -0.39×10^{-6} of M_{Ar}. The fractional uncertainty of the molar mass was assessed to be the same as the work in [8], 0.7×10^{-6}, because the same reference isotopic reference gas, the same mass spectrometer, and the same method of analysis were used.

7. Conclusions

Table 3 and figure 5 summarize the determinations of the molar masses of five lots of commercially-manufactured, high-purity argon. Figure 5 suggests that the acoustic measurements and the mass-spectroscopy measurements agree within combined uncertainties. To express this agreement quantitatively, we consider the three ratios: $M_{\mathrm{A}}/M_{\mathrm{A(1)}}$, $M_{\mathrm{C}}/M_{\mathrm{C(1)}}$, and $M_{\mathrm{C}}/M_{\mathrm{C(2)}}$ and we recall that Samples C(1) and C(2) had very different histories; therefore, their mass measurements were uncorrelated. We find the average $(\langle M_{\mathrm{acoustic}}/M_{\mathrm{mass\text{-}spec}}\rangle - 1) = (-0.31 \pm 0.69) \times 10^{-6}$, where the indicated uncertainty is one standard deviation; therefore, it does not include the larger, Type B uncertainties of the acoustic and mass-spectroscopy references discussed above. The difference is well covered by the claimed uncertainties with the acoustic comparison and the gravimetric mass-spectrometry [8]. The agreement is indeed remarkable.

Acknowledgments

We thank Laurent Pitre of LNE-CNAM for his helpful suggestions for conducting good measurements and Allan Harvey of NIST for his helpful suggestions for improving this manuscript. This work was supported by the National Key Research and Development Project of China (no.2016YFF0200101) and the National Natural Science Foundation of China (nos. 51476153 and 51276175). Feng Xiaojuan thanks the Young Elite Scientist Sponsorship Program (YESS) by CAST for support.

Appendix. Mass dependence of the second acoustic virial coefficient

When we replaced equation (3) with equation (4) above, we assumed that the acoustic virial coefficients of Ar40 and those of commercially-purchased, high-purity argon were identical. To our knowledge, the calculations of argon's virial coefficients have not accounted for the very small differences between the virial coefficients between the various isotopes. Here, we provide order-of-magnitude estimates to justify our assumption.

For a first estimate, we follow Hirschfelder *et al* [16] in using the Lennard–Jones (L–J) model interatomic potential

$$\varphi(r) = 4\varepsilon\left[\left(\frac{\sigma}{r}\right)^{12} - \left(\frac{\sigma}{r}\right)^{6}\right], \tag{A.1}$$

where, for argon, $\sigma = 0.34\,\mathrm{nm}$ is the distance at which the potential crosses zero and $\varepsilon/k_{\mathrm{B}} = 122\,\mathrm{K}$ is the depth of the potential well. Using the numerical data in Hirschfelder *et al*'s tables I-A and I-E, we calculated the classical, mass-independent, second density virial coefficient $B_{\mathrm{class}}(T)$ from $\varphi(r)$. We also calculated the first quantum correction to $B(T)$, which is proportional to $(\Lambda^*)^2$, where $\Lambda^* \equiv h/[\sigma(m\varepsilon)^{1/2}]$ is the de Broglie wavelength of the relative motion of two atoms with relative kinetic energy ε, h is Plank's constant, and m is the mass of an atom. The results are:

$$B(273\,\mathrm{K}) = [-22.65 + 0.14\,(M/40\ \mathrm{g \cdot mol^{-1}})]\ \mathrm{cm^3 \cdot mol^{-1}}. \tag{A.2}$$

The same L–J potential has the acoustic virial coefficient and pressure coefficient

$$\begin{aligned} B_{\mathrm{acoustic}}(273\,\mathrm{K}) &= [4.64 + 0.16\,(M/40\ \mathrm{g \cdot mol^{-1}})]\,\mathrm{cm^3 \cdot mol^{-1}} \\ A_1(273\,\mathrm{K}) &= 10^{-4} \times [6.13 + 0.21\,(M/40\ \mathrm{g \cdot mol^{-1}})]\,(p/300\,\mathrm{kPa}). \end{aligned} \tag{A.3}$$

These L–J results are reasonably close to the experimental values: $B(273\,\mathrm{K}) = -21.20\,\mathrm{cm^3 \cdot mol^{-1}}$ and $B_{\mathrm{acoustic}}(273\,\mathrm{K}) = 5.40\,\mathrm{cm^3 \cdot mol^{-1}}$ [17].

In the present work, the average molar mass of the Ar40 reference gas is larger than that of the other argon samples by the fraction 0.000 368. Therefore, we estimate that the mass-dependent part of $A_1 p$ at 273 K and 300 kPa changes by the very small amount: $0.21 \times 10^{-4} \times 3.68 \times 10^{-4} = 0.77 \times 10^{-8}$.

The L–J calculation of $B(T)$ started with the mass-independent inter-atomic potential equation (A.1). Our second estimate considers the question: how does the mass-dependence of the potential itself affect $B(T)$? To our knowledge, this question has not been answered for argon. However, Cencek *et al* [18] calculated the helium–helium interaction potential $V(R)$ (in their notation) as a function of the distance between the helium nuclei for both ^{4}He and ^{3}He and

they used their potential to calculate thermophysical properties including the second acoustic virial coefficients ^{4}He and ^{3}He. They calculated an approximate, infinite-nuclear-mass, (Born–Oppenheimer) potential $V_{BO}(R)$ and many corrections to $V_{BO}(R)$. At high temperature the effects of statistics (Bose for ^{4}He; Fermi for ^{3}He) are unimportant and the largest correction is the adiabatic correction $V_{ad}(R)$ that accounts for the finite mass of the nucleus. For values of the ^{4}He–^{4}He potential in the range $100\ \mathrm{K} \leqslant V/k_B \leqslant 100\,000\ \mathrm{K}$, Cencek *et al* find V_{ad}:$V_{BO} \approx 1{:}3000 \approx$ (mass of 2 electrons):(mass of 4 nucleons) $= 1{:}3670$. This helium result suggests that an *upper bound* to the adiabatic correction for argon will be of the order of (mass of 20 electrons):(mass of 40 nucleons) $= 1{:}3670$. However, a much smaller adiabatic correction seems likely for argon. If we approximate the repulsive part of $V_{Ar,BO}(R)$ by an L–J potential with, for example $\varepsilon/k_B = 122\ \mathrm{K}$ and $\sigma = 0.34\ \mathrm{nm}$, we expect the adiabatic correction to increase ε/k_B by $(122\ \mathrm{K})/3670 = 33$ mK. In the present work, we compared mixtures of argon isotopes which differ in average atomic mass by 0.037%. We estimate that the differences between the adiabatic corrections for these mixtures is equivalent to 0.037% of 33 mK, a truly insignificant 12 μK.

References

[1] Moldover M R, Trusler J P M, Edwards T J, Mehl J B and Davis R S 1988 *J. Res. Natl. Bur. Stand.* **93** 85–144

[2] de Podesta M, Underwood R, Sutton G, Morantz P and Harris P 2013 *Metrologia* **50** 354–76

[3] Pitre L, Risegari L, Sparasci F, Plimmer M D, Himbert M E and Albo P A G 2015 *Metrologia* **52** S263–73

[4] Pitre L, Sparasci F, Truong D, Guillou A, Risegari R and Himbert M E 2011 *Int. J. Thermophys.* **32** 1825–86

[5] Gavioso R M, Ripa D M, Steur P P M, Gaiser C, Truong D, Guianvarc'h C, Tarizzo P, Stuart F M and Dematteis R 2015 *Metrologia* **52** S274–304

[6] Sutton G, Underwood R, Pitre L, de Podesta M and Valkiers S 2010 *Int. J. Thermophys.* **31** 1310–46

[7] Lin H, Feng X J, Gillis K A, Moldover M R, Zhang J T, Sun J P and Duan Y Y 2013 *Metrologia* **50** 417–32

[8] Yang I, Pitre L, Moldover M R, Zhang J T, Feng X J and Kim J S 2015 *Metrologia* **52** S394–409

[9] Trusler J P M 1991 *Physical Acoustics and Metrology of Fluids* (London: Taylor and Francis)

[10] Gillis K A and Moldover M R 1996 *Int. J. Thermophys.* **15** 821–46

[11] Lee J Y, Marti K, Severinghaus J P, Kawamur K, Yoo H S, Lee J B and Kim J S 2006 *Geochim. Cosmochim. Acta* **70** 4507–12

[12] Volkiers S, Vendelboa D, Berglunda M and de Podesta M 2010 *Int. J. Mass Spectrom.* **291** 41–7

[13] Mark D F, Stuart F M and de Podesta M 2011 *Geochim. Cosmochim. Acta* **75** 7494501

[14] Zhang J T, Lin H, Feng X J, Sun J P, Gillis K A, Moldover M R and Duan Y Y 2011 *Int. J. Thermophys.* **32** 1297329

[15] Nier A 1950 *Phys. Rev.* **77** 789–93

[16] Hirschfelder J O, Curtiss C F and Bird R B 1954 *Molecular Theory of Gases and Liquids* (New York: Wiley)

[17] Lemmon E W, McLinden M O and Huber M L 2010 *REFPROP: Reference Fluid Thermodynamic and Transport Properties* NIST Standard Reference Database 23, Version 9.1, (Boulder, CO: National Institute of Standards and Technology) www.nist.gov/srd/nist23.cfm

[18] Cencek W, Przybytek M, Komasa J, Mehl J B, Jeziorski B and Szalewicz K 2012 *J. Chem. Phys.* **136** 224303